Brain signatures indexing variation in internal processing during perceptual decision-making

Johan Nakuci[1*], Jason Samaha[2] and Dobromir Rahnev[1]

[1]School of Psychology, Georgia Institute of Technology, Atlanta, Georgia, 30332, USA.
[2]Department of Psychology, The University of California, Santa Cruz, Santa Cruz, California, 95064, USA.

*Corresponding author. Email: jnakuci3@gatech.edu

Acknowledgments: This work was supported by the National Institutes of Health (grant R01MH119189 to DR) and the Office of Naval Research (grant N00014-20-1-2622 to DR).

Author contributions:
Conceptualization: JN, DR
Methodology: JN, DR
Data Curation: JS
Visualization: JN, JS, DR
Funding acquisition: DR
Writing – original draft: JN, DR
Writing – review & editing: JN, JS, DR

Competing interests: Authors declare that they have no competing interests.

Abstract

Meaningful variation in internal states remains challenging to discover and characterize. Using modularity-maximation, a data-driven classification method, we identify two subsets of trials with distinct spatial-temporal brain activity and differing in the amount of information required to reach a decision. These results open a new way to identify brain states relevant to cognition and behavior not associated with experimental factors.

Main Text

Brain activity is highly variable during simple and cognitively demanding tasks[1,2] impacting performance[3,4]. This variability is present in the activity of individual neurons[5] up to changes among large-scale neural networks[6]. Discovering, characterizing, and linking variability in brain activity to internal processes has primarily relied on experimentally inducing changes (e.g., via attention manipulation) to identify neuronal and behavioral consequences[7] or studying spontaneous changes in ongoing brain dynamics[8]. However, changes in internal processing could arise from many factors, such as variation in strategy or arousal[9] that are independent of experimental conditions but are relevant to cognition and behavior[10]. Moreover, traditional approaches often rely on knowing, a priori, what features of brain activity (e.g., oscillations) or cognition (e.g., attention) are relevant to measure or manipulate.

Here, we leverage a data-driven approach to characterize the variability in brain activity among individual trials and link this variability to behavior and underlying latent cognitive processes. Subjects performed a motion discrimination task where they judged the global direction of a set of moving dots (left/right) with six levels of coherence (**Fig. 1A**). Even in a simple task such as this, trial-to-trial spatial and temporal variation in brain activity measured with electroencephalography (EEG) is evident (**Fig. 1B**).

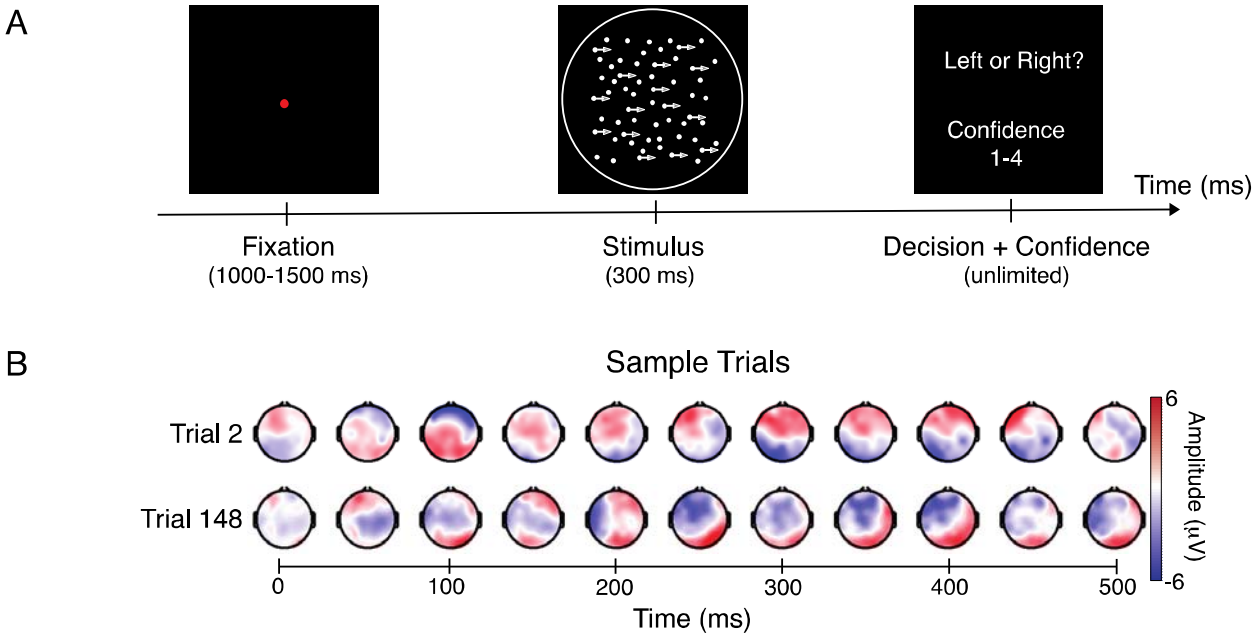

Figure 1. Task description and trial-to-trial spatial-temporal variation. A) Subjects viewed a dot motion stimulus for 300 ms with net motion direction either to the left or the right at varying levels of motion coherence (arrowed dots). Using a single button press, subjects provided a choice and confidence (1-4) judgment. B) EEG activity from two trials from stimulus onset (0 ms) to 500 ms after onset from the same subject. The brain activity between the trials exhibits stark differences.

We explore the link between trial-to-trial variation and decision-making processes using a data-driven classification method we developed previously[11]. Briefly, modularity-maximization is used to identify consistent patterns of activity among trials[12]. Trials from all subjects were pooled together to calculate the spatial and temporal similarity using Pearson correlation from stimulus onset (0 ms) to 500 ms after onset. The modularity-maximization classification procedure identified two subgroups of trials, Subtype 1 (N_{trials} = 10674) and Subtype 2 (N_{trials} = 10284; **Fig. 2A**), across all subjects (**Fig. 2B**).

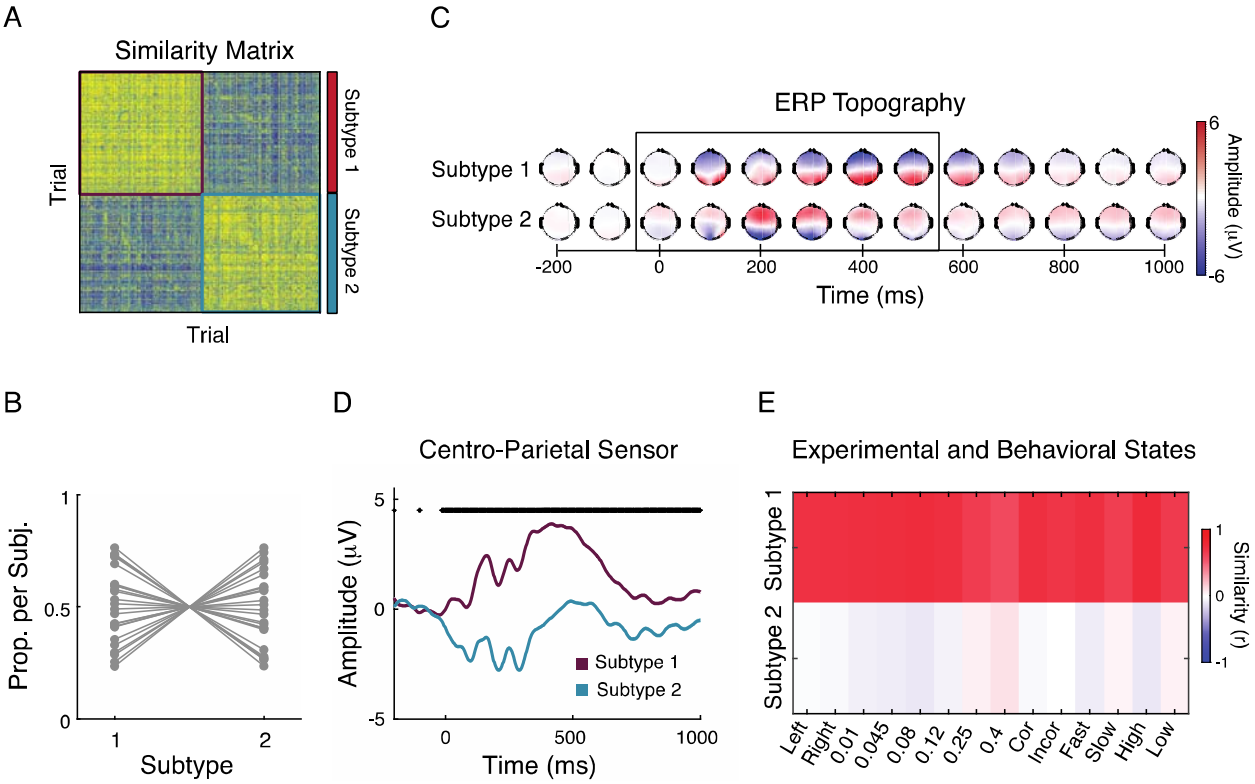

Figure 2. Subtypes of individual trials in motion perception task. A) Modularity-maximization based clustering identified two subtypes of trials, Subtype 1 and Subtype 2. The colored squares correspond to the trials composing each subtype. Pearson correlation was used to calculate the spatial-temporal similarity of the EEG activity among individual trials from 0 to 500 ms post-stimulus. B) The proportion of trials in each subject classified as either subtype 1 or 2. C) ERP topographies of Subtype 1 and Subtype 2 from 200 ms before stimulus onset to 1000 ms after stimulus offset. Note that the clustering algorithm was applied to the data from stimulus onset (0 ms) to 500 ms, black box. D) ERP activity from the centro-parietal sensor per subtype. Each waveform shows the mean (thick line) and standard error of the mean (shaded area). Statistical testing was conducted using independent samples t-tests, and FDR corrected for multiple comparisons. Statistically significant differences in amplitude are marked at the top of the panel. E) The topographical similarity between subtype-derived ERPs to ERPs derived from experimental – motion direction (Left/Right), motion coherence (0.01, 0.045, 0.08, 0.12, 0.25 0.4) – and behavior factors – Correct/Incorrect response, Fast/Slow response time, High/Low confidence. Pearson correlation was used to calculate the spatial-temporal similarity of the EEG activity from individual trials for 0 to 1000 ms after the stimulus. The ERP from one of the subtypes, Subtype 1, exhibits strong similarity ($r > 0.60$) to ERPs derived from experimental and behavioral factors highlighting the utility of Modularity-Maximization based clustering to identify variation in internal processing relevant to cognition.

To understand the nature of the two subtypes, we plotted their average event-related potentials (ERPs) to test for differences in stimulus-driven activity[13]. Qualitatively, the ERPs for each

subtype exhibited an opposite pattern of anterior vs. posterior event-related potentials (**Fig. 2C**). These qualitative topographical differences were present even when comparing ERPs for each motion coherence level (**Fig. S1A, B).** To confirm these impressions, we compared ERPs from the centro-parietal sensor, which has been linked with decision-making processes[14] and evidence accumulation[15,16]. Significant differences were present in amplitude between the subtypes (independent samples t-tests, $p < 0.001$, FDR corrected; **Fig. 2D**) and for each motion coherence level (independent samples t-tests $p < 0.001$, FDR corrected; **Fig. S1C**). Subtype 1 contained significant positive amplitude in the parietal area compared to Subtype 2 from stimulus onset (0 ms) to 1000 ms after the stimulus extending beyond the 500 ms window used in the clustering.

One possibility is that these subtypes reflect different experimental or behavioral factors, such as leftward/rightward moving trials or fast/slow responses. To better assess the nature of these subtypes, we compared the topographical similarity between subtype-derived ERPs to ERPs derived by averaging trials associated with experimental (motion direction and coherence levels) and behavioral (accuracy, response times, and confidence) factors. The topographical similarity was estimated between ERPs from stimulus onset (0 ms) to 1000 ms after the stimulus. Interestingly, a strong similarity was found in Subtype 1 ($r > 0.60$), but not in Subtype 2 ($r < 0.10$) to ERPs derived from experimental and behavioral factors, indicating that the variation in the stimulus-locked ERP in 43% of trials in our study were induced by other factors (**Fig. 2E**).

We then investigated if these differences between the two subtypes were due to underlying differences in the composition of trials. The distribution of trials with leftward and rightward motion was the same between subtypes (Wilcoxson rank sum test: $Z = 0.13$; $p = 0.89$; **Fig. S2A**).

Although Subtype 1 contained a higher proportion of trials with lower motion coherence (Wilcoxson rank sum test: $Z = -4.06$; $p = 4.72 \times 10^{-5}$; **Fig. S2B**), this difference accounted for less than 3% of trials per condition (**Fig. S2C)**. Thus, experimental factors were not the main driver of the spatial-temporal variation in brain activity among trials.

However, the subtypes reflect alterations in underlying cognitive and decision-making processes. Subtype 1 trials consistently exhibited faster response times across all motion coherence levels (independent samples t-test: $t(20956) = -6.97$; $p = 3.29 \times 10^{-12}$; **Fig. 3A, Fig. S2A)**. On the other hand, there was no significant difference between the two subtypes in accuracy (independent samples t-test: $t(20956) = 1.35$; $p = 0.17$; **Fig. 3B, Fig. S2B)**, and only marginally higher confidence in Subtype 1 trials (independent samples t-test: $t(20956) = 1.79$; $p = 0.07$; **Fig. 3C, Fig. S2C).**

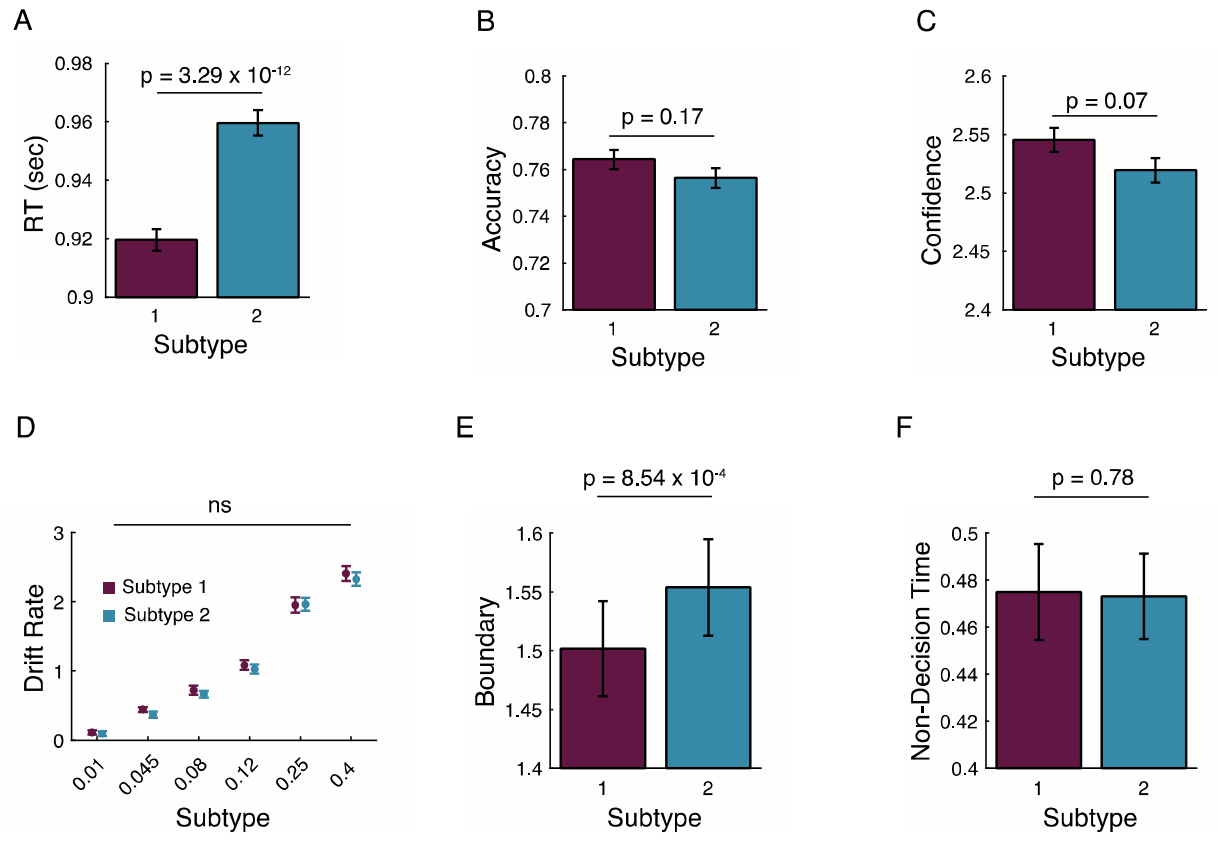

Figure 3. Behavioral differences between subtypes. Differences in (A) response times, (B) accuracy, and (C) confidence between subtypes. Error bars show the mean ± sem. Drift-diffusion parameters showed that (D) the drift rate was the same between subtypes, (E) the response boundary was higher in Subtype 2, and (F) the non-decision time exhibited no differences between subtypes. Statistical testing was conducted using independent samples t-tests, and FDR corrected for multiple comparisons. ns = not significant

Having identified two trial subtypes with underlying differences in stimulus-dependent brain activity and decision-making processes, we sought to identify the latent cognitive processes that would give rise to the behavioral differences by computationally modeling the response times and accuracy using the drift-diffusion model[17]. We fit the drift-diffusion model to the behavioral data from each subtype separately. We let the drift rate vary with motion coherence level, but the decision boundary and non-decision time were fixed across the different coherence levels. Examining the latent factors, we found the drift rate was the same between subtypes (independent samples t-test; $p > 0.05$; **Fig. 3D)**, but Subtype 2 trials featured significantly higher

response boundary (independent samples t-test: t(24) = -3.81; p = 0.001; **Fig. 3E)**. Further, no differences were present in the non-decision time (independent samples t-test: t(24) = 0.28; p = 0.81; **Fig. 3F).**

To ensure our results are generalizable and robust, we conducted two additional analyses. First, we trained a Support Vector Machine (SVM) classifier by randomly separating trials into 5 bins containing 20% of trials. The classifier was trained on EEG data from four of the bins (80% of trials) and tested on the remaining bin (20% of the trials). The procedure was repeated until each bin was tested. The SVM classifier correctly predicted subtype labels with greater than 98% accuracy (**Fig. S4**). Second, we replicated the analysis using a longer time window (1000 ms) to verify that the results were not dependent on the time range used in the clustering analysis. The classification similarity between the 500 ms and 1000 ms time windows was strong (>84%; **Fig. S5A-C)** which is reflected in the ERP and behavioral analysis (**Fig. S5D-O)**.

Through a combination of data-driven classification of brain activity, behavior, and computational modeling, we identify two brain states with differing stimulus-driven activity. These states reflect changes in latent cognitive factors which could indicate different modes of processing during perceptual decision-making in humans[18] and other animals[19]. These modes could arise from changes in a single information processing sequence induced by alteration in the balance between top-down[20] and bottom-up signaling[21]. Alternatively, the different stimulus-driven activity could indicate the existence of two independent information processing sequences. Taken together, the analytical approach and findings open a new avenue for understanding the brain-behavior relationship**.**

References

1. Arieli, A., Sterkin, A., Grinvald, A. & Aertsen, A. *Science (1979)* (1996).doi:10.1126/science.273.5283.1868
2. Goris, R.L.T., Movshon, J.A. & Simoncelli, E.P. *Nat Neurosci* (2014).doi:10.1038/nn.3711
3. Reinhart, R.M.G. & Nguyen, J.A. *Nat Neurosci* **22**, 820–827 (2019).
4. Mišić, B., Mills, T., Taylor, M.J. & McIntosh, A.R. *J Neurophysiol* **104**, 2667–2676 (2010).
5. Ribrault, C., Sekimoto, K. & Triller, A. *Nat Rev Neurosci* (2011).doi:10.1038/nrn3025
6. Clare Kelly, A.M., Uddin, L.Q., Biswal, B.B., Castellanos, F.X. & Milham, M.P. *Neuroimage* (2008).doi:10.1016/j.neuroimage.2007.08.008
7. Renart, A. & Machens, C.K. *Curr Opin Neurobiol* **25**, 211–220 (2014).
8. Samaha, J., Iemi, L., Haegens, S. & Busch, N.A. *Trends Cogn Sci* **24**, 639–653 (2020).
9. Fontanini, A. & Katz, D.B. *J Neurophysiol* (2008).doi:10.1152/jn.90592.2008
10. Waschke, L., Kloosterman, N.A., Obleser, J. & Garrett, D.D. *Neuron* **109**, 751–766 (2021).
11. Nakuci, J., Covey, T.J., Shucard, J.L., Shucard, D.W. & Muldoon, S.F. *bioRxiv* 2022.05.03.490545 (2022).doi:10.1101/2022.05.03.490545
12. Mucha, P.J., Richardson, T., Macon, K., Porter, M.A. & Onnela, J.P. *Science (1979)* (2010).doi:10.1126/science.1184819
13. Luck, S.J. (Steven J. *The MIT Press* (2014).doi:10.1118/1.4736938
14. Ratcliff, R., Philiastides, M.G. & Sajda, P. *Proceedings of the National Academy of Sciences* **106**, 6539–6544 (2009).
15. Parés-Pujolràs, E., Travers, E., Ahmetoglu, Y. & Haggard, P. *Neuroimage* **232**, 117863 (2021).
16. Twomey, D.M., Murphy, P.R., Kelly, S.P. & O'Connell, R.G. *European Journal of Neuroscience* **42**, 1636–1643 (2015).
17. Ratcliff, R. & McKoon, G. *Neural Comput* **20**, 873–922 (2008).
18. Weilnhammer, V., Stuke, H., Standvoss, K. & Sterzer, P. *bioRxiv* 2021.08.20.457079 (2022).doi:10.1101/2021.08.20.457079
19. Ashwood, Z.C. et al. *Nat Neurosci* **25**, 201–212 (2022).
20. Zanto, T.P., Rubens, M.T., Thangavel, A. & Gazzaley, A. *Nat Neurosci* **14**, 656–661 (2011).
21. Mechelli, A., Price, C.J., Friston, K.J. & Ishai, A. *Cerebral Cortex* **14**, 1256–1265 (2004).
22. Delorme, A. & Makeig, S. *J Neurosci Methods* (2004).doi:10.1016/j.jneumeth.2003.10.009
23. Jeub, L.G.S., Bazzi, M., Jutla, I.S. & Mucha, P.J. (2011).at <http://netwiki.amath.unc.edu/GenLouvain, https://github.com/GenLouvain/GenLouvain>
24. Bassett, D.S. et al. *Chaos* (2013).doi:10.1063/1.4790830